

Magnetic susceptibility and electrical resistivity of LaMnO_3 , CaMnO_3 , and $\text{La}_{1-x}\text{Sr}_x\text{MnO}_3$ ($0.13 \leq x \leq 0.45$) in the temperature range 300–900 K

J. A. Souza,¹ J. J. Neumeier,¹ R. K. Bollinger,¹ B. McGuire,¹ C. A. M. dos Santos,^{1,2} and H. Terashita¹

¹*Department of Physics, Montana State University, P.O. Box 173840, Bozeman, Montana 59717-3840, USA*

²*Escola de Engenharia de Lorena—USP, P.O. Box 116, Lorena, São Paulo 12602-810, Brazil*

(Received 8 January 2007; revised manuscript received 27 March 2007; published 6 July 2007)

Measurements of the magnetic susceptibility χ and electrical resistivity ρ are reported in the temperature range 300–900 K for $\text{La}_{1-x}\text{Sr}_x\text{MnO}_3$, with $x=0, 0.13, 0.20, 0.25, 0.35$, and 0.45 , and for CaMnO_3 . The main focus of this work is to develop a better understanding of the Curie-Weiss paramagnetism and the temperature-independent contributions to the magnetic susceptibility due to Pauli (χ_{Pauli}) and Van Vleck paramagnetism. Measurements of the electrical resistivity in the same temperature range were conducted to learn about the electrical conduction mechanisms, and whether or not charge carriers are present which might contribute to χ_{Pauli} .

DOI: [10.1103/PhysRevB.76.024407](https://doi.org/10.1103/PhysRevB.76.024407)

PACS number(s): 75.47.Lx, 71.30.+h, 75.50.Ee, 75.47.Gk

I. INTRODUCTION

Perovskite manganese oxides have been studied extensively in the last 12 years because they exhibit an unusually large magnetoresistance as well as charge and magnetic ordering. These effects are believed to arise due to strong coupling among the charge, lattice, and spin (magnetic) degrees of freedom. It is well known that the magnetic susceptibility is anomalous¹ in the region near the ferromagnetic transition temperature T_c . This has led to difficulties in studying the critical behavior associated with the magnetic transition.² In addition, most studies of manganese oxides have focused on phenomena occurring below 400 K where magnetic and electronic transitions such as colossal magnetoresistance occur. Orbital order-disorder and structural phase transitions are known to exist at higher temperatures.³ Moreover, magnetic-susceptibility measurements above 400 K are scarce in the literature.^{4–6} With magnetic transition temperatures in some of these compounds above 300 K, it is difficult with the available data to learn about the variety of terms contributing to the paramagnetic susceptibility and the nature of the precursors of long-range-ordered states at low T . In this paper, measurements of magnetic susceptibility and electrical resistivity are presented in the temperature range 300–900 K. Contributions to paramagnetic susceptibility originating from localized ions and itinerant carriers are discussed for antiferromagnetic (AFM) CaMnO_3 and LaMnO_3 and ferromagnetic (FM) Sr-doped LaMnO_3 .

II. EXPERIMENT

Two polycrystalline samples of nominal composition LaMnO_3 were prepared using standard solid-state reaction. For one sample ($\text{LaMnO}_{3.02}$), all reactions were conducted under Ar atmosphere. The second sample ($\text{LaMnO}_{3.04}$) was reacted in air followed by a final reaction in a flow of Ar and a mixture of reduction gas of H_2/N_2 (3% H_2). Sr-doped samples of $\text{La}_{1-x}\text{Sr}_x\text{MnO}_3$ with $x=0.13, 0.20, 0.25, 0.35$, and 0.45 and CaMnO_3 were also prepared using standard solid-state reaction in air. X-ray powder diffraction confirmed the single-phase nature for all samples. Four-probe electrical re-

sistivity was measured in flowing Ar gas using a homemade apparatus with a platinum thermometer mounted close to the sample; silver epoxy was used to make contacts to the specimens. Magnetization measurements from room temperature to 900 K were performed using a vibrating-sample magnetometer from Quantum Design at high vacuum. Data were collected on warming to the highest temperature followed by cooling to check for changes in magnetic susceptibility associated with loss of oxygen or irreversible structural changes. The average Mn oxidation state was determined by iodometric titration. The titration procedure was repeated at least three times for each sample; the resulting values and uncertainties⁷ are listed in Table I.

III. ELECTRICAL RESISTIVITY

Although the main focus of this work is the magnetic susceptibility above 300 K in perovskite manganese oxides, during the course of this work it became apparent that measurements of the electrical resistivity in the same temperature range would assist in understanding the various contributions to the magnetic susceptibility.

Figure 1 shows the electrical resistivity for $\text{CaMnO}_{2.97}$. The measurement was performed warming the sample to 850 K [curve (1) in Fig. 1] followed by cooling and warming again in a flow of Ar. Magnetic susceptibility of this same sample was measured (see Fig. 1) to 900 K *prior* to the resistivity measurement; heating to 900 K caused the oxygen content to change from 3.00 to 2.97. A first-order semiconductor-metallic-like transition with robust hysteresis takes place at T_S , the orthorhombic to rhombohedral structural phase transition.³ Reversibility of $\rho(T)$ in subsequent runs indicates that the metallic state in the rhombohedral phase is not related to changes in the Mn oxidation state. It is interesting that the coexistence of orthorhombic and rhombohedral phases extends over a very large temperature interval, $\Delta T=80$ K, as observed in both magnetic (see below) and resistivity data. The charge carriers in CaMnO_3 are known to be large polarons, in contrast to small polarons in the hole-doped manganese oxides.⁸ This point is illustrated in the inset of Fig. 1 where inspection reveals that the small-polaron

TABLE I. Values of Mn^{4+} concentration, T_C or T_N , effective magnetic moment p_{eff} , χ_{VV} , and $|\chi_{\text{core}}|$.

Sample	Mn^{4+}	$T_{C,N}$ (K)	θ (K)	p_{eff} (μ_B)	χ_{VV}^a	$ \chi_{\text{core}} ^b$
$\text{LaMnO}_{3.02}$	0.040(3)	139	63/168 ^b	5.30(4)/5.34(4) ^b	0.55(5)	0.66
$\text{LaMnO}_{3.04}$	0.069(6)	133	80/180	5.51(4)/5.26(4)	0.55(5)	0.66
$x=0.13$	0.171(8)	270	359	4.70(3)	0.54(5)	0.65
$x=0.20$	0.217(9)	323	384	4.66(3)	0.53(5)	0.64
$x=0.25$	0.275(6)	350	399	4.65(3)	0.52(5)	0.64
$x=0.35$	0.336(6)	367	404	4.59(3)	0.51(5)	0.63
$x=0.45$	0.466(3)	355	382	4.62(3)	0.49(5)	0.63
$\text{CaMnO}_{2.97}$	0.947(7)	124	-499/-239	4.39(4)/4.03(3)	0.41(5)	0.59

^aMagnetic susceptibilities are in units of 10^{-4} emu/mol Oe.

^bBelow/above T_{JT} or T_S .

hopping model, $\ln(\rho/T) = \ln(A) + E_p/k_B T$ (E_p is the polaron hopping energy), is not satisfied. The slight oxygen deficiency creates electron-doped carriers through the introduction of Mn^{3+} ions. The decrease in resistivity above T_S is probably associated with the reduction of the lattice distortion (orthorhombic strain) across T_S . This change in crystal structure probably reduces the energy gap. As a result, above T_S the available thermal energy is sufficient to excite the charge carriers to the conduction band, or to impurity states within the band gap, leading to a metalliclike temperature dependence of $\rho(T)$.

Although electrical resistivity at high temperature for LaMnO_3 has been reported in the literature,^{6,9} we measured our sample for additional characterization. The electrical resistivity was reported to be temperature independent⁶ above the Jahn-Teller orbital order disorder transition T_{JT} , a behavior suggested to result from charge transport by vibronic carriers.⁶ Optical conductivity measurements¹⁰ reveal a gap

in the electronic structure of LaMnO_3 below T_{JT} which closes above. Band-structure calculations also reveal this gap.¹¹ The closing of a gap and the addition of itinerant charge carriers might lead to a Pauli paramagnetic contribution above T_{JT} .

Figure 2 shows the electrical resistivity for $\text{LaMnO}_{3.02}$. The measurement was performed on warming the sample to 890 K followed by cooling in constant Ar flow. A sharp decrease in the electrical resistivity occurs at the Jahn-Teller orbital order-disorder transition $T_{JT}=718$ K (warming curve). The cooling curve shifts to slightly lower temperature ($T_{JT}=710$ K), which is associated with the first-order nature¹² of the transition but may also be affected by a slight loss of oxygen. It is interesting that the hysteresis near T_{JT} is far less pronounced than in $\text{CaMnO}_{2.97}$.

The electrical resistivity of hole-doped manganites follows the polaron hopping model, $\ln(\rho/T) = \ln(A) + E_p/k_B T$, where E_p is the polaron hopping energy, k_B is the Boltzmann constant, and the prefactor $A \approx k_B/e^2 a_p^2 n_p \omega_{op}$, with e the charge of the carrier, a_p the polaron hopping distance, n_p the

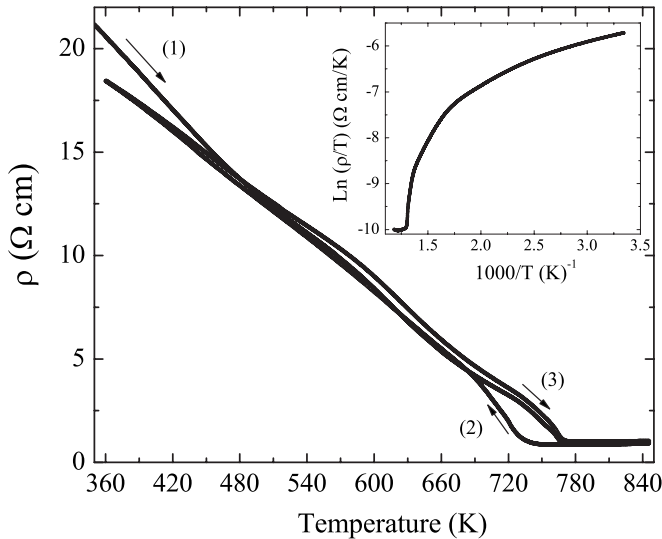


FIG. 1. Electrical resistivity as a function of temperature for $\text{CaMnO}_{2.97}$. The measurements were done warming to 850 K [curve labeled (1)] followed by cooling (2) and warming (3) again. The inset displays $\ln(\rho/T)$ versus $1000/T$ (warming curve) illustrating that the resistivity does not obey the small-polaron model.

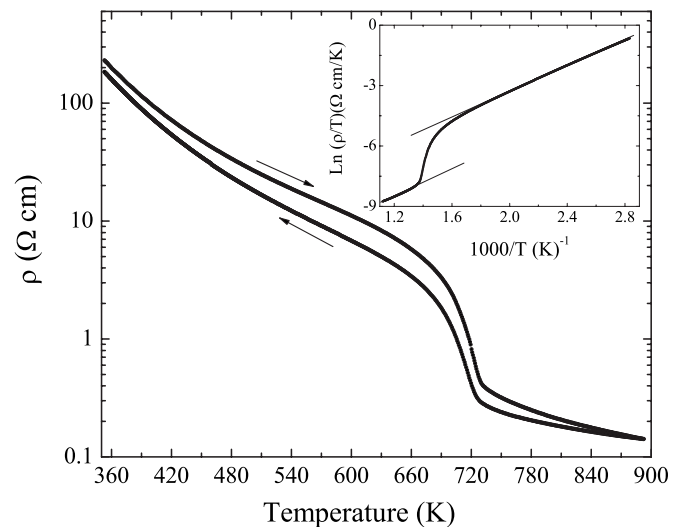


FIG. 2. Electrical resistivity as a function of temperature for $\text{LaMnO}_{3.02}$ warming and cooling. The inset shows $\ln(\rho/T)$ versus $1000/T$ (only the cooling curve) describing the small-polaron model.

carrier density, and ω_{op} the optical phonon frequency.^{13,14} The inset of Fig. 2 indicates that $\rho(T)$ is very well described by the polaron model above and below T_{JT} . Our observation that the polaron hopping energy is identical, $E_p=0.29(1)$ and $0.28(1)$ eV, above and below T_{JT} is consistent with a prior report⁹ on $\text{La}_{0.95}\text{Sr}_{0.05}\text{MnO}_3$ which has a Mn^{4+} concentration similar to the 4% of our sample. In addition, our value $T_{JT}=718$ is lower than stoichiometric^{6,9} LaMnO_3 , which is also consistent with the depression of T_{JT} with increased Mn^{4+} concentration.⁹ The prefactor A is about 20 times smaller above T_{JT} . This is probably a result of a larger hopping distance a_p due to the reduced number of Jahn-Teller distorted sites¹⁵ and perhaps an increase in the carrier density; phonon frequencies do not change significantly¹⁶ at T_{JT} , so ω_{op} is assumed constant. A key point is that rather than free charge carriers as in a metal, they are polaronic in nature. This will have importance in our analysis of the magnetic susceptibility.

IV. MAGNETIC SUSCEPTIBILITY

At high temperatures, the magnetic susceptibility of localized noninteracting magnetic ions along with charge carriers can be written as

$$\chi(T) = \frac{C}{T - \theta} + \chi_{core} + \chi_{VV} + \chi_{Pauli}. \quad (1)$$

The first term is the Curie-Weiss contribution, where C and θ are the Curie and Weiss constants, respectively. The Curie constant is $C = Np_{eff}^2\mu_B^2/3k_B$, where N is the density of magnetic ions, k_B is the Boltzmann constant, and μ_B is the Bohr magneton. The effective magnetic moment, neglecting spin-orbital coupling, can be obtained using $p_{eff} = g\sqrt{xS_1(S_1+1) + (1-x)S_2(S_2+1)}$, where $g=2$ is the Landé factor and $S_1=3/2$ and $S_2=2$ for Mn^{4+} and Mn^{3+} , respectively.

The temperature-independent contribution χ_{core} is associated with diamagnetism of filled electronic shells of the core ions. The values for our specimens, calculated using a published tabulation,¹⁷ are given in Table I. These were added to our data prior to further analysis, since $\chi_{core} < 0$. Van Vleck (VV) susceptibility χ_{VV} originates from transitions between ground-state and excited orbitals in ions with partially filled electronic shells. It is also temperature independent. An expression derived by Lines¹⁸ for Ni, which has a cubic crystal field structure similar to Mn, is given by $\chi_{VV} = 8N\mu_B^2/\Delta$, where Δ is the energy gap between the ground-state (t_{2g}) and excited (e_g) levels. Octahedral crystal-field splitting decreases with increasing Mn-O distance; typical values for Mn^{4+} , Mn^{3+} , and Mn^{2+} containing oxides are 2.5, 1.8, and 1 eV, respectively.^{19,20} Using this equation and $\Delta=2.5$ (1.8) eV for CaMnO_3 (LaMnO_3), one obtains $\chi_{VV}=0.56$ (0.41×10^{-4}) emu/mol Oe.²³ Using the appropriate ratio of Mn^{3+} to Mn^{4+} , the values provided in Table I are estimated for each of the measured samples; these values were subtracted from our measurement data prior to further analysis.

With the presence of charge carriers, a Pauli paramagnetic contribution should result. It is given by $\chi_{Pauli} = \chi_P$

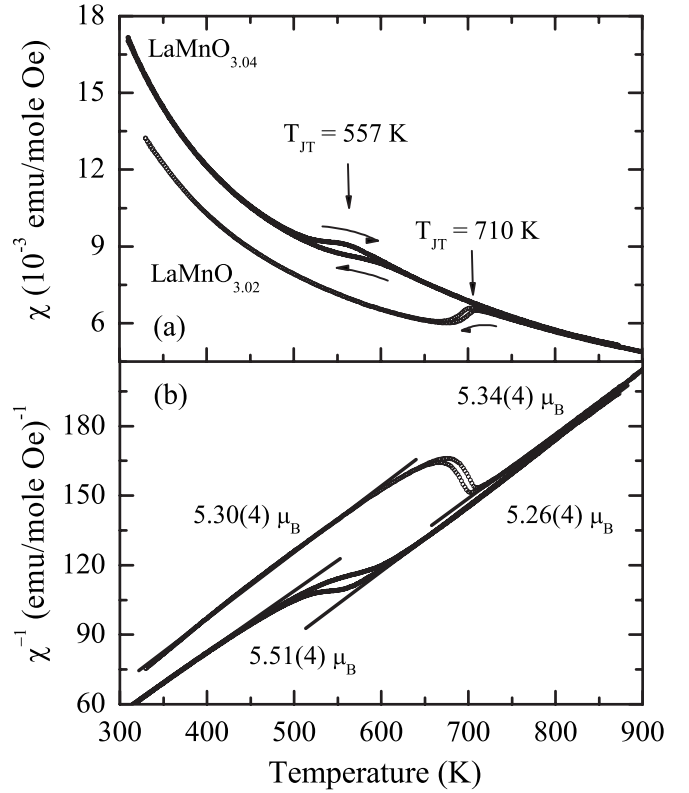


FIG. 3. (a) Magnetic susceptibility and (b) its inverse as a function of temperature for $\text{LaMnO}_{3.04}$ and $\text{LaMnO}_{3.02}$.

$(1 - \chi_1 T^2)$, where $\chi_P = (1/2)g^2\mu_B^2N(E_F)$. $N(E_F)$ is the density of states at the Fermi energy E_F and $\chi_1 = \pi^2/12(k_B/E_F)^2$. The term quadratic in T is often neglected, but it might become significant at high temperatures. It arises from the second-order Sommerfeld expansion of the chemical potential.²¹ The diamagnetic Landau contribution for metals is typically $-1/3\chi_{Pauli}$. If the effective mass of the carriers is enhanced, for example, through coupling with the lattice, this contribution can be neglected. The possibility of a χ_{Pauli} term in our samples will be discussed below.

Stoichiometric LaMnO_3 contains Mn^{3+} magnetic ions that order with an A-type antiferromagnetic structure.²² The values of T_N for our $\text{LaMnO}_{3.02}$ and $\text{LaMnO}_{3.04}$ samples are shown in Table I. They are in good agreement with the expected values.²⁴ Figure 3(a) displays the magnetic-susceptibility data as a function of temperature for these samples. Both exhibit a Jahn-Teller phase transition where orbitally ordered e_g orbitals become disordered^{6,15,25} above $T_{JT}=710$ K for $\text{LaMnO}_{3.02}$. With an increase in oxygen content, T_{JT} is shifted to lower temperature.^{5,6} Our $\text{LaMnO}_{3.04}$ sample exhibits $T_{JT}=557$ K. This transition is clearly visible in Fig. 3(a). Simultaneous to the distinct change in the magnetic susceptibility at T_{JT} , a dramatic decrease of the electrical resistivity takes place; however, it is polaroniclike above and below T_{JT} . As a result, we do not expect a Pauli paramagnetic term (which is associated with free charge carriers). The expected effective paramagnetic moment is $p_{eff} = 4.86$ and $4.83 \mu_B$ for $\text{LaMnO}_{3.02}$ and $\text{LaMnO}_{3.04}$, respectively. Our results indicate that p_{eff} is higher (7–10 %) than expected for spin-only localized moments, indicating that another contribution to $\chi(T)$ exists.

Another observation suggesting the lack of a χ_{Pauli} term comes from considering the temperature dependence of χ . The addition of a positive temperature-independent contribution, such as χ_{Pauli} , adds curvature to χ^{-1} , but also increases the effective magnetic moment. Thus, the enhancement of p_{eff} could, in principle, arise from Pauli paramagnetism. However, p_{eff} is essentially the same above and below T_{JT} for $\text{LaMnO}_{3.02}$ and smaller above T_{JT} than below for $\text{LaMnO}_{3.04}$. Thus, even though a dramatic change in the itinerant nature of the charge carriers occurs above T_{JT} , our magnetic-susceptibility data rule out the appearance of a discernible Pauli susceptibility. This observation leads to the possibility that charge disproportionation ($2\text{Mn}^{3+} = \text{Mn}^{2+} + \text{Mn}^{4+}$) takes place above T_{JT} , as suggested by Zhou and Goodenough.⁶ This mechanism would imply that the polarons are less localized and the average effective paramagnetic moment should be the same, above and below T_{JT} .

To further study the susceptibility magnitude, the Weiss constants θ are obtained for each sample (see Table I). While the Curie constant is the same below and above T_{JT} for $\text{LaMnO}_{3.02}$, the Weiss constant changes from 63 to 168 K above T_{JT} . The Weiss constants for $\text{LaMnO}_{3.04}$ are 80.0 K below T_{JT} and 180 K above. Thus, even though the samples have almost the same susceptibility magnitude above T_{JT} , slightly different Weiss constants indicate that the differing $\text{Mn}^{3+}/\text{Mn}^{4+}$ ratios influence the microscopic magnetic interaction above and below T_{JT} . The positive value of θ obtained below T_{JT} is related to the presence of FM interaction in the *ab* plane and AFM along the *c* axis.²² The differences in the magnetic susceptibility for $\text{LaMnO}_{3.04}$ and $\text{LaMnO}_{3.02}$ can be understood in the following manner. Below T_{JT} , the larger θ of $\text{LaMnO}_{3.04}$ enhances χ . This is caused by an increase in FM correlations below T_{JT} that also lead to the slightly larger p_{eff} . Above T_{JT} , both specimens have the same χ and p_{eff} values as a result of charge disproportionation.⁶

CaMnO_3 orders antiferromagnetically with *G*-type antiferromagnetic structure.^{22,26} Figure 4 shows magnetic susceptibility from 320 to 900 K. The measurement was performed increasing the temperature from room temperature to 900 K followed by cooling to 320 K and warming again to 900 K. At 600 K, there is loss of oxygen, as observed in the data [first run labeled (1)], and an irreversible character of the curves (first and second runs). When increasing the temperature (third run), the data follow the cooling curve and the transition is reversible as observed in Fig. 4. After these runs, the sample was titrated to obtain the average Mn oxidation state. The Mn^{4+} concentration was 0.947(7), resulting in $\text{CaMnO}_{2.97}$. Magnetic susceptibility measured on a second sample reproduced the results. Electrical resistivity measurements on this second sample are shown in Fig. 1. Figure 4(b) shows a deviation of experimental data from the Curie-Weiss behavior at $T \sim 400$ K. We believe that this is due to the presence of a secondary magnetic phase associated with oxygen defects. For example, $\text{CaMnO}_{2.5}$ shows an antiferromagnetic transition around $T_N \sim 350$ K.²⁷

At high temperatures, a structural phase transition $T_S = 750$ K, from orthorhombic to pseudocubic rhombohedral, takes place for $\text{CaMnO}_{2.97}$. It is interesting to note that the hysteresis associated with that transition is large, reaching $\Delta T = 80$ K. Clearly, this structural transition is first order in

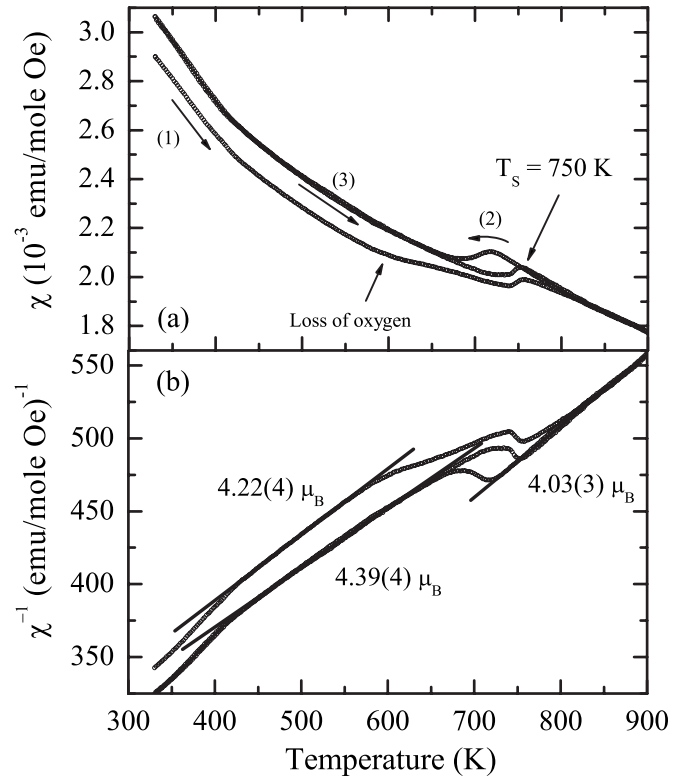


FIG. 4. (a) Magnetic susceptibility and (b) its inverse as a function of temperature for $\text{CaMnO}_{2.97}$.

nature. The expected effective paramagnetic moment for $\text{CaMnO}_{2.97}$ is $p_{eff} = 3.93 \mu_B$, which is smaller than observed in Fig. 4. As in our LaMnO_3 samples, the enhanced p_{eff} suggests that another contribution should be subtracted from the data. It is important to note that above T_S , the effective magnetic moment is smaller than below (by 8.2%) in a very similar fashion to that observed in $\text{LaMnO}_{3.04}$ which decreases by 4.5%. This similarity suggests that the average lattice structure plays a role in both $\text{CaMnO}_{2.97}$ and $\text{LaMnO}_{3.04}$, since the samples have higher crystallographic symmetry above T_S and T_{JT} . Although p_{eff} is larger than expected, the electrical resistivity is indicative of a behavior typical for doped semiconductors with a small carrier concentration. For this reason, we assume that χ_{Pauli} is negligible.

The magnetic susceptibility for five hole-doped samples of $\text{La}_{1-x}\text{Sr}_x\text{MnO}_3$ ($x = 0.13, 0.20, 0.25, 0.35,$ and 0.45) is shown in Fig. 5. Data were collected on warming to the highest temperature followed by cooling to check for changes in magnetic susceptibility associated with loss of oxygen; none were observed except for $x = 0.35$ where a small amount of hysteresis ($\Delta T = 8$ K, in the temperature range 550–780 K) was observed. Magnetic-susceptibility measurements at high temperatures (up to 800 K) for some similar compositions have been reported³⁰ ($x \leq 0.20$), but our measurements and analysis extend the composition range and temperature range (by 100 K) and consider contributions from diamagnetism, Van Vleck paramagnetism, and Pauli paramagnetism.

Figure 6 shows χ^{-1} versus T for four of the $\text{La}_{1-x}\text{Sr}_x\text{MnO}_3$ specimens after subtraction of the temperature-independent

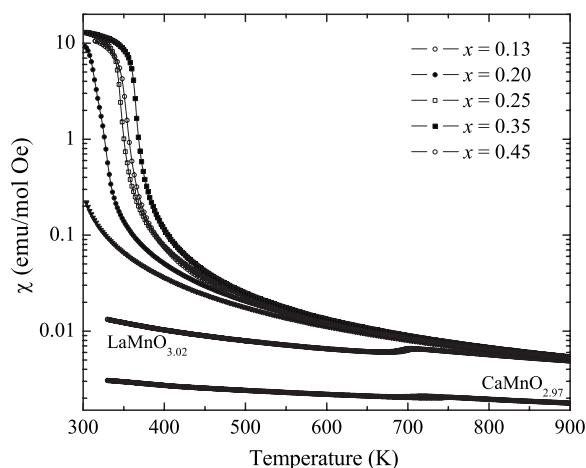


FIG. 5. Magnetic susceptibility as a function of temperature for the doped samples with $x=0.13$, 0.20 , 0.25 , 0.45 , 0.35 , and 0.45 . The data of LaMnO_3 and CaMnO_3 are also included for comparison.

terms (χ_{core} and χ_{VV}). The hole-doped samples show χ values that are larger than those of $\text{CaMnO}_{2.97}$ and $\text{LaMnO}_{3.02}$. This is related to the magnitude of the Weiss temperatures θ (see below). The curves are not linear over the whole paramagnetic temperature range, revealing that the Curie-Weiss term in Eq. (1) cannot fully account for the behavior of χ^{-1} versus T . A departure from linear behavior clearly sets in below 600 K. This is in agreement with a prior report²⁸ on $x=0.33$ and may be associated with short-range magnetic order due to the formation of magnetic polarons.²⁹ The Weiss temperature for each sample is shown in Table I. The values are larger than the Curie temperature, indicating strong ferromagnetic correlations. Both the presence of short-range order and high values of θ are sufficient to understand the higher value of $\chi(T)$ observed in the Sr-doped samples relative to $\text{CaMnO}_{2.97}$, $\text{LaMnO}_{3.02}$, and $\text{LaMnO}_{3.04}$. The effective magnetic moments (p_{eff}) are obtained by fitting the data in the temperature range 700–900 K. The values of p_{eff} for samples with $x=0.13$ – 0.35 are in good agreement with the expected values for a spin-only system as shown by the solid line in the lower inset of Fig. 6. However, the sample with $x=0.45$ exhibits a larger than expected p_{eff} .

In order to estimate the temperature-independent contribution, clearly pronounced for $x=0.45$, the Curie constant is constrained to yield the effective magnetic moment expected for this $\text{Mn}^{4+}/\text{Mn}^{3+}$ ratio. This is valid given the strong Hund's coupling of the e_g electron in Mn^{3+} . Using the ratio $\text{Mn}^{3+}/\text{Mn}^{4+}$ (see Table I), a constant of 2.2×10^{-4} emu/mol Oe is subtracted out to obtain the expected value of $p_{\text{eff}}=4.45 \mu_B$ for $x=0.45$. We attribute this contribution to Pauli paramagnetism. Using this value, a density of states $N(E_F)=2.0 \times 10^{24}$ eV⁻¹ mol⁻¹ is obtained. This value is in agreement with that obtained through heat-capacity measurements.^{32,33} In addition, we have measured heat capacity at low temperature on this sample (not shown). If one assumes that the linear term in the heat capacity arises entirely from the presence of charge carriers, one can calculate

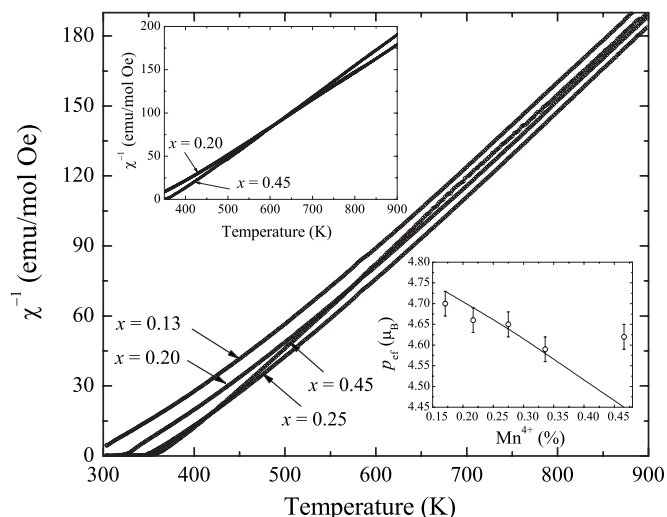


FIG. 6. χ^{-1} versus T for Sr-doped samples with nominal concentrations of $x=0.13$, 0.20 , 0.25 , and 0.45 . The upper inset shows the warming and cooling curves of χ^{-1} for $x=0.20$ and 0.45 . The lower inset shows the obtained effective magnetic moment for the doped samples and the solid line indicates the expected values.

$N(E_F)=1.1 \times 10^{24}$ eV⁻¹ mol⁻¹. This value is close to that obtained from the χ measurements. Thus, we believe that it is reasonable that the $x=0.45$ sample exhibits a Pauli paramagnetic term, while the samples with $x \leq 0.35$ do not. This difference arises from the change from insulating to low-resistivity metallic behavior at $x > 0.25$ due to increased carrier concentration.³¹

V. CONCLUSIONS

In summary, measurements of magnetic susceptibility and electrical resistivity are reported in the temperature range 300–900 K. Electrical resistivity suggests that $\text{LaMnO}_{3.02}$ is polaronic in nature above and below T_{JT} in agreement with $\chi(T)$, while in $\text{CaMnO}_{2.97}$ the small-polaron model is not satisfied. Above T_S , $\text{CaMnO}_{2.97}$ shows a metalliclike behavior, probably due to thermal excitation of charge carriers; however, no Pauli contribution is observed in $\chi(T)$ after correcting for diamagnetic and Van Vleck contributions. The Sr-doped specimens, with the exception of $x=0.45$, show no Pauli paramagnetism as well. In the case of $x=0.45$, an appreciable temperature-independent contribution is observed. This is attributed to Pauli paramagnetism associated with the observed metallic electrical behavior. The Sr-doped specimens reveal curvature in χ^{-1} below 600 K that is likely associated with the formation of short-range magnetic order (polarons).

ACKNOWLEDGMENTS

This material is based upon work supported by the Brazilian agencies CNPq (Grant No. 201017/2005-9), CAPES (Grant No. 0466/05-0), the National Science Foundation (Grant No. DMR-0504769), and the U.S. DOE, Office of Basic Energy Sciences (DE-FG-06ER46269).

- ¹M. Zeise, *J. Phys.: Condens. Matter* **13**, 2919 (2001).
- ²D. Kim, B. L. Zink, F. Hellman, and J. M. D. Coey, *Phys. Rev. B* **65**, 214424 (2000).
- ³V. Kiryukhin, *New J. Phys.* **6**, 155 (2004).
- ⁴S. B. Oseroff, M. Torikachvili, J. Singley, S. Ali, S.-W. Cheong, and S. Schultz, *Phys. Rev. B* **53**, 6521 (1996).
- ⁵M. Tovar, G. Alejandro, A. Butera, A. Caneiro, M. T. Causa, F. Prado, and R. D. Sanchez, *Phys. Rev. B* **60**, 10199 (1999).
- ⁶J.-S. Zhou and J. B. Goodenough, *Phys. Rev. B* **60**, R15002 (1999).
- ⁷The titration experiment determines the average Mn valence under the assumption that the valences of La, Sr, Ca, and O are +3, +2, +2, and -2. It is well known that these Mn oxides possess La and Mn defects rather than an oxygen excess. In this work, the average Mn valence is stated explicitly or in a formula such as LaMnO_{3+y} , neglecting the possibility of defects.
- ⁸J. L. Cohn, C. Chiorescu, and J. J. Neumeier, *Phys. Rev. B* **72**, 024422 (2005).
- ⁹P. Mandal, B. Bandyopadhyay, and B. Ghosh, *Phys. Rev. B* **64**, 180405(R) (2001).
- ¹⁰K. Tobe, T. Kimura, Y. Okimoto, and Y. Tokura, *Phys. Rev. B* **64**, 184421 (2001).
- ¹¹D. V. Efremov and D. I. Khomskii, *Phys. Rev. B* **72**, 012402 (2005).
- ¹²T. Chatterji, F. Fauth, B. Ouladdiaf, P. Mandal, and B. Ghosh, *Phys. Rev. B* **68**, 052406 (2003).
- ¹³N. F. Mott and E. A. Davies, *Electron Processes in Non-Crystalline Materials* (Clarendon, Oxford, 1979).
- ¹⁴M. Jaime, H. T. Hardner, M. B. Salamon, M. Rubinstein, P. Dorsey, and D. Emin, *Phys. Rev. Lett.* **78**, 951 (1997).
- ¹⁵J. Rodriguez-Carvajal, M. Hennion, F. Moussa, A. H. Moudden, L. Pinsard, and A. Revcolevschi, *Phys. Rev. B* **57**, R3189 (1998).
- ¹⁶L. Martín-Carrón and A. de Andrés, *Eur. Phys. J. B* **22**, 11 (2001).
- ¹⁷Landolt-Bornstein, New Series, Group II, Vol. 16, edited by K.-H. Hellwege and A. M. Hellwege (Springer-Verlag, Heidelberg, 1986).
- ¹⁸M. E. Lines, *Phys. Rev.* **164**, 736 (1967).
- ¹⁹E. Dagotto, T. Hotta, and A. Moreo, *Phys. Rep.* **344**, 1 (2001).
- ²⁰J. M. D. Coey, M. Viret, and S. V. Molnar, *Adv. Phys.* **48**, 167 (1999).
- ²¹N. W. Aschcroft and N. D. Mermin, *Solid State Physics* (Saunders College, Philadelphia, 1988).
- ²²E. O. Wollan and W. C. Koehler, *Phys. Rev.* **100**, 545 (1955).
- ²³The uncertainties are estimated taking into account variations in the values (Refs. 19 and 20) of Δ .
- ²⁴Y. Tokura, *Rep. Prog. Phys.* **69**, 797 (2006).
- ²⁵E. Granado, J. A. Sanjurjo, C. Rettori, J. J. Neumeier, and S. B. Oseroff, *Phys. Rev. B* **62**, 11304 (2000).
- ²⁶E. Granado, C. D. Ling, J. J. Neumeier, J. W. Lynn, and D. N. Argyriou, *Phys. Rev. B* **68**, 134440 (2003).
- ²⁷K. R. Poeppelmeier, M. E. Leonowicz, and J. M. Longo, *J. Solid State Chem.* **44**, 89 (1982); E. Bakken, J. Boerio-Goates, T. Grande, B. Hovde, T. Norby, L. Rormark, R. Stevens, and S. Stolen, *Solid State Ionics* **176**, 2261 (2005).
- ²⁸M. T. Causa, M. Tovar, A. Caneiro, F. Prado, G. Ibanez, C. A. Ramos, A. Butera, B. Alascio, X. Obradors, S. Pinol, F. Rivadulla, C. Vazquez-Vazquez, A. Lopez-Quintela, J. Rivas, Y. Tokura, and S. B. Oseroff, *Phys. Rev. B* **58**, 3233 (1998).
- ²⁹J. Tanaka, H. Nozaki, S. Horiuchi, and M. Tsukioka, *J. Phys. (Paris)* **44**, L129 (1983).
- ³⁰M. Paraskevopoulos, F. Mayr, J. Hemberger, A. Loidl, R. Heichele, D. Maurer, V. Müller, A. A. Mukhin, and A. M. Balbashov, *J. Phys.: Condens. Matter* **12**, 3993 (2000).
- ³¹A. Urushibara, Y. Moritomo, T. Arima, A. Asamitsu, G. Kido, and Y. Tokura, *Phys. Rev. B* **51**, 14103 (1995).
- ³²J. M. D. Coey, M. Viret, L. Ranno, and K. Ounadjela, *Phys. Rev. Lett.* **75**, 3910 (1995).
- ³³A. Michalopoulou, E. Syskakis, and C. Papastaikoudis, *J. Phys.: Condens. Matter* **15**, 7763 (2003).